Computer Tomograph Measurements in Shear and Gravity Particle Flows

B. Dencs[1], J. Szepvolgyi[1], P. Bogner[2], T. Foldes[3], and J. Gyenis[1]

[1] University of Kaposvar, Research Institute of Chemical & Process Engineering, Egyetem u. 2., H-8200, Veszprem, Hungary

[2] University of Kaposvar, Institute of Diagnostics, Guba S. u. 40, H-7400 Kaposvar, Hungary

[3] Hungarian Oil and Gas Co., Ady E. u.26 , H-5000 Szolnok, Hungary

Abstract

The paper reports the recent results obtained on the applicability of cross-sectional digital imaging method to study particle flow characteristics in 3D particle beds forced to move by gravity or shear. X-ray CT imaging technique is widely used in medical diagnostics and, during the last decades, its spatial and temporal resolution has been improved significantly. In this study, an attempt was made to use this technique for engineering purposes. Two experimental set-ups with different types of particle flows were investigated using Siemens Somatom Plus type CT equipment. A series of trials were carried out in a small model hopper with flat bottom and almost cylindrical side wall slightly deviating from verticality. Non steady-state flow was studied during the outflow of particulate material from this vessel, through a central hole at the bottom. Further investigation was fulfilled in a modified Cuette-type shearing device to study steady-state shear flow. This equipment consisted of an almost cylindrical vessel identical to that used for gravity flow measurements, and a smaller inner cylinder rotating within this vessel concentrically, around its vertical axis. The surface of the inner cylinder was notched vertically, i.e. perpendicularly to the direction of rotation to increase wall friction between the particles and the cylinder. Almost spherical sucrose granules, also used for gravity flow measurements, were filled into the gap between the rotating cylinder and the outer wall of the equipment. Movement of particles took place due to shear, generated within the particle bed. By using X-ray CT technique, cross-sectional digital images were obtained in every two seconds for both types of particle flows. For this, the cross-sectional variation of the local Hounsfield density values were measured in a matrix of *0.1x0.1x2.0 mm* space elements. It was proved that the applied non-invasive cross-sectional imaging technique was suitable to distinguish the stationary and moving particle regions, and by this, to estimate the location of the boundary zone between them.

Key words: granular flow, X-ray computer tomography, particle bed

1. Introduction

The applied measurement technique is based on the principle of computer tomography, utilizing the phenomena of X-ray (or γ-ray) absorption [1]. It is well known that the extent of the attenuation of radiation depends on the thickness, density and chemical nature of the investigated material, this latter being characterized by X-ray absorption coefficient.

It means that if constant energy of irradiation is ensured, the intensity of the transmitted energy depends exclusively on the properties of material being in the path of radiation. In CT equipment, the weakened X-ray beams arrive at a series of detectors producing electric signals depending on the intensity of radiation transmitted to them. During data acquisition, these detectors are turning

around the investigated object, thus performing several hundreds or thousands of measurements. The X-ray intensity data measured by this way are used for the computation of X-ray absorption coefficients for each predefined location of the studied body, arranged into a matrix. According to the measured absorption coefficients, different graduation values are attributed to these locations, given by Hounsfield Units (HU). In a modified Hounsfield-scale defined by the OSIRIS evaluation software used by us, vacuum and water have zero and 1024 HU values, respectively. Other materials of various compositions are characterized by HU values proportional with their absorption coefficients [2]. Rendering a user defined gray-scale or color palette to different Hounsfield values, very informative images can be produced from various respects.

Recently, besides medical application, CT technique is increasingly used for technical purposes, too. An interesting application is non-destructive examination of oil and gas reservoir rocks. Foldes et al. [3] reported their results of CT measurements for 3D reservoir characterization.

Bartholomew and Casagrande [4] were the first who applied X-ray absorption tomography to measure the concentration of solid particles in gas-fluidized systems. Recently, Martin et al. [5] used this technique to determine the cross-sectional distribution of solids suspension in circulating fluidized bed in a 0.94 m ID industrial FCC riser. Chester et al. [6] have studied the mixing dynamics of solid particles in double-cone blenders by using X-ray absorption CT technique.

Besides X-ray absorption, other highly developed cross-sectional imaging methods are also used to study the structure of solids materials. Sederman et al. [7-9] applied Magnetic Resonance Imaging (MRI) volume-visualization technique to determine the characteristics of liquid flow and pore structures of packed beds. It was pointed out that transport processes occurring within the void spaces of a solid material are of fundamental importance to many process operations, such as oil recovery from rock formations and remediation of non-aqueous phase liquid contaminated soil. The structure of packed beds influences the heat transfer within the packing itself, as well as the mass transfer, the pressure drop and heterogeneity of fluid flow within the void spaces.

Besides applying γ-ray absorption, George et al. [10] used electrical impedance tomography to study the material distribution in vertical three-phase flow. Mann et al. [11-12] studied mixing process by electrical resistance tomography. Dyakowski et al. [13] reviewed the application of various electrical resistance (or impedance) tomography (ERT) and capacitance tomography (ECT) to study various the flow systems of particulate materials. In the past few years, ECT was widely used to study particulate systems. Papers have been published on solids flow imaging and attrition studies [14], real time visualization of dense phase powder conveying [15], particle detection [16] and real time flow structures in gas-liquid and gas-liquid-solid systems [17].

Ultrasonic process tomography is also promising technique to study the structure of particulate solids, as was described and applied by Schlaberg, Podd and Hayle [18].

2. Experimental

During the work reported here, two different systems were investigated by X-ray computer tomography. Gravity flow of particles in a small model hopper, discharging through a central bottom hole, was studied under non steady-state conditions. In another system, quasi steady-state particle motion was induced around a rotating inner cylinder in a Cuette-type shearing device.

The first system, used for gravity flow measurements, was a small circular perspex model hopper with flat bottom, having a slight conicity with 3.1^o side angle. Main dimensions were as follows: I.D. *88 mm* at the bottom and *100 mm* at the top. Its total height was *110 mm* filled with material to *100 mm*. In the middle of bottom plate, a circular discharging hole took place with *15 mm* diameter. The vessel was open above, to facilitate the outflow of particles without any gas stream through the particle bed. Flow was started by opening the outlet hole by a remote mechanism.

For flow measurements, nearly spherical sucrose granulates were used with of $790\ kg/m^3$ bulk density, having *1.4 mm* average diameter and narrow size distribution between *1,25-1,60 mm*. The angle of repose was 40.9^o.

The second series of experiments were carried out on shear flow, which was induced in a modified Cuette-type shearing device somewhat differing from that used earlier by Tardos et al. [19]. It consisted of an almost cylindrical stationary vessel, identical to that used for gravity flow measurements, and a smaller inner cylinder rotating within this vessel concentrically around its vertical axis. Diameter and height of the rotating cylinder were *52 mm* and *80 mm*, respectively. For this study, its rotation speed was set to *80 rpm*. The surface of this inner cylinder was notched vertically, i.e. perpendicularly to the direction of rotation, in order to increase the wall friction between the particles and the cylinder. Nearly spherical sucrose granulates, identical to those used for gravity flow experiments, were filled into the gap between the rotating cylinder and the outer wall of the equipment. Movement of particles took place due to shear generated by the rotating cylinder within the bed. The free upper surface of particle bed above, as well as the slight conicity of the equipment wall facilitated to accommodate the particle bed within the available space during shearing.

By X-ray computer tomography technique, cross-sectional digital images were obtained for both types of flow systems, using Siemens Somatom Plus type equipment. This installation allowed two modes of operation: it could produce single image on a slice along a given cross section of the studied object, or it could be programmed to obtain multiple images on several slices. The position of slices can be continuously shifted along a predetermined length of the measured object applying spiral mode operation, or can be fixed to one position to produce repeated measurements on a given cross-section. For the purposes of the study reported here, especially because of the non steady-state nature of particle flow in the first series of experiments, generally identical slices were measured and evaluated along the middle vertical cross-section of the vessel repeatedly.

In some cases, spiral mode operation was also applied, to discover the whole bed structure and particle movements in other cross sections, too. Because the studied particle systems were axially symmetrical, these latter measurements gave no significant additional information till now. It will be probably more important if quantitative data will be needed on the paths of individual tracer particles.

The applied imaging algorithm corresponded to *2 seconds* cycle time and *2 mm* slice width. Data matrix referring to one cross-section contained HU values for *512x512* locations at a time, i.e. the density data of *512x512=262,144* space elements, called data matrix cells, were determined. According to the applied *2 mm* slice width and *0.1x0.1 mm* cross-sectional resolution, the dimensions of one matrix cell were *0.1x0.1x2.0 mm*.

To investigate the non-steady state gravity flow, measurements started just before opening the discharging hole and were continued till the time when the flow was ceased. At this final stage, only a part of material formed a slanting heap, corresponded to the dynamic angle of repose, remained in the hopper between the edge of the central hole and the outer wall. To study the sheared particle bed in the Cuette-type device, only a few measurements were carried out at the central vertical cross-section. Due to the continuous and quasi steady-state operation, it proved to be enough to obtain representative images on the particle bed.

During the experiments reported here, the measured density values of matrix cells were changing between zero (air in void spaces) and about 1800, this latter corresponding to the relative density of sucrose granules.

Primer evaluation of data was made by OSIRIS medical software, elaborated by a team at the University of Geneva [20]. Built in data processing capability of this software could result in statistical data along a selected line or area of CT image, designated as a Region of Interest (ROI). By this, histograms of pixel brightness values, the minimal, maximal and average density values, as well as standard deviation could be obtained. Further data processing and analysis were made by usual statistical methods.

3. Results and discussion

Resulting images

Some representative pictures on the central vertical cross-section of the studied model hopper are shown in *Fig.1*, obtained by X-ray CT imaging technique, at different time instants of repeated measurements on the non steady-state outflow of particles. From these, it can clearly be seen the changing upper contours of the particle bed, as well as the inner structure of the stationary regions, outside of the central funnel shaped moving region. Bright pixels (high density points) correspond to the material of solid particles, while black pixels (low density points) represent the void spaces between them. In these pictures, the area of the moving particle regions can be well distinguished from the stagnant zones, because of the diffuse outlines and lower brightness of the images or traces of the moving particles. This is probably due to the displacements of these particles during the time of one imaging cycle, i.e. when the tube detectors were still turning. Supposing that solids flow in the studied model hopper is axially symmetrical, the displacements of particles are probably almost parallel to the measured central vertical slice.

Similar qualitative information can be read from the picture obtained for the particle bed sheared in the studied Cuette-type equipment, shown in *Fig.2*. On this Figure, three different regions can be well distinguished:

a.) A region of particles close to the vertical surface of the rotating cylinder, which were moving more or less together with the surface of this cylinder, i.e. mainly tangentially. Some vertical downward motion could also be supposed here from observation of animated series of repeated CT images. Pictures of particles being in this region have rather diffuse contours and less bright pixel points.

b.) Another kind of flow could be supposed around the lower edge (or corner) of the rotating cylinder, causing even less brightness and more diffuse particle contours. It can either be

attributed to higher tangential velocity and/or certain whirling flow of particles, due to the composed effects of the vertical surface and the lower horizontal face of the rotating cylinder.

c.) The outer region of particle bed shows sharper particle images, supposedly corresponding to practically immobile particles. However, at the vicinity of the outer wall, diffuse particle contours and lower brightness indicate certain displacements. Animated series of repeated CT images revealed a slow upward motion here, causing some vertical circulation of particles within the gap. (Slow upward flow at the outer stationary wall, and slow downward motion at the rotating cylinder). But, the extent of this vertical circulation is much less then particle movements discussed in paragraphs *a* and *c*.

Quantitative evaluation of CT images

Statistical evaluation of pixel brightness values or HU density levels along a line, or in a selected area (Roi = Region of Interest) allows to obtain quantitative information on the given part of an object. This can be utilized to render the qualitative observations, described above, more exact. As an example, *Fig.3* shows a representative CT image on particle bed during discharge from the studied model hopper. Stationary zones in this Figure were marked by Roi-3 and Roi-4, while Roi-5 corresponds to flowing region. Histograms on the frequency of various density levels within the stationary and flowing zones are shown in *Fig4a* and *Fig4b*, respectively.

From these histograms, the following statements can be done: The distribution of HU density levels has higher maximum (about $1.5x10^{-3}$) within the flowing region, located at lower density (at about *730*). In the stationary zone, these values are about $1.3x10^{-3}$ and *880*, respectively. This difference is also manifested by the computed mean values of HU densities, being *760* in the flowing and *830* in the stationary particle regions. Standard deviation was much lower for the flowing region (*304*) than in the stationary zones (361), although their relative values compared to the mean values are close to each other (40.0 % and 43.5 %, respectively).

It also has to be noticed that these histograms are bimodal, as obtained originally from OSIRIS image processing software. It means that, in addition to the maximum mentioned above, there is another maximum at zero density, not shown in these diagrams. It corresponds to the frequency of pixel points, which are falling to the area of void spaces. The mean density values and standard deviations, referred above, were calculated by discarding this second maximum. For this respect, pixel points falling into the images of solid particles were only taken into account. However, in comparing the stationary and moving particle zones, frequency difference of black pixel points is also characteristic. Namely, their relative frequency in the stationary region is about three times higher than in the flowing region ($29.5\ x10^{-3}$ and $10.9x10^{-3}$, respectively).

In CT image taken on the vertical cross-section of the studied Cuette-type shearing device, some characteristic regions are marked in *Fig 5*. These regions, similarly to the pictures taken on gravity flow are also differing, in respect of pixel point brightness distribution and particle sharpness. Notations of Roi-1, 2, 5 and 6 represent particle regions, which are moving together in some extent with the rotating cylinder. Roi-3, 4 and 7 refer to more or less stationary regions. Based on the distributions of pixel brightness levels, some qualitative assessments could also be done on these regions. Cumulative distribution curves of these regions are shown on *Fig.6*.

From *Fig 5*, as was mentioned already, it can be clearly seen that particle regions close to the vertical surface of the rotating cylinder (Roi-1 and 2) have less bright pixels and more diffuse contours. Cumulative distribution functions confirm this qualitative observation, because they are shifted toward the black end of the brightness scale, and are steeper than distribution functions relating to stationary regions Roi-3 and 4. This result is similar to that obtained for gravity flow, discussed above, where the mean brightness values and their standard deviation were also lower in the moving regions. Distribution functions obtained for the almost stationary regions Roi-3 and 4 show broader distribution (less steep cumulative distribution), which is also in good agreement with the results obtained for gravity flow. These curves are shifted towards the white end of the scale, also indicating that their mean values are higher, i.e. these pixel points are generally brighter. Moving particle region at the lower edge of the rotating cylinder (Roi-5 and 6), have the steepest distribution, also shifted toward the white end of the scale. This latter means higher mean brightness value, which can not be totally explained till now, but it may be caused by the probably higher particle velocity in this region both in perpendicular and transverse directions. Particle region just below the lower face of rotating cylinder (Roi-7) has similar characteristics to stationary regions Roi-3 and 4, except at higher brightness values, where the distribution curve shows somewhat lower frequencies, indicating certain displacement of particles here.

Quantitative statistical analysis was also made along several lines drawn vertically within the stationary (Roi-3 and 4) and moving (Roi-1 and 2) regions. Some characteristic results are shown in *Table 1*. Similarly to the results discussed above, this analysis also confirmed that the mean pixel brightness and standard deviation are significantly lower in the moving particle regions compared to the stationary zones. However, there is no characteristic difference in the relative standard deviation, because standard deviations were proportional with the mean values. All these observations are in good agreement with the results obtained for gravity flow measurements discussed above.

Table 1. Characteristic data of brightness distributions along vertical lines in various particle bed regions in Cuette-type shearing device

Characteristic brightness data	Roi-1,2 moving region	Roi-3,4 stationary region
Mean value	793.3	887.4
Std. deviation	302.8	354.4
Relative std. deviation	38.2 %	39.9 %

Characteristic features can be discovered by comparing phase space portraits or attractors of the brightness values changing along these vertical lines. *Figs. 7a* and *b* show the brightness values of (*i*-1)th pixel points in HU density units as a function of those of *i*th pixel points in the stationary and moving particle regions, respectively. Significant difference can be observed between the surface areas covered by these space portraits, as well as in their maximal brightness values. From these Figures, it can be clearly seen that both the covered surface area and their maximal extension are reduced significantly, comparing the moving particle regions to the stationary zones.

These differences obtained by quantitative analysis of cross-sectional CT images of the studied particle beds, in addition to qualitative observation, can give useful tool to distinguish the moving and stationary regions, and to estimate the location of their bordering surfaces.

4. Conclusions

In this paper, a study on the applicability of X-ray CT imaging technique to discover particle flow structure or characteristics was reported. Two flow systems were investigated: non steady-state gravity outflow from a small model hopper, and quasi steady-state shear flow around a rotating cylinder in a modified Cuette-type device.

Qualitative observation of cross-sectional CT images showed well determined differences between the stationary and moving particle regions in both systems, making also possible to estimate the borders between these zones. Brightness values of the CT images or traces of individual particles were differing probably due to their displacement during the measurement. The higher was the translation velocity of particles, the less brightness with more diffuse contours was obtained for them. Quantitative analysis of brightness value distributions of CT image pixel points also showed characteristic differences. Mean brightness values in the moving particle regions were definitely lower with smaller standard deviation, compared to the stationary regions. However, relative standard deviation did not show significant differences because of the more or less proportionality of standard deviation with the mean values. Statistical analysis of brightness distribution along various vertical lines drawn within these regions showed similar quantitative differences.

It has to be noticed that the applied technique did not give direct quantitative data on the exact particle velocities or velocity field. But, in further studies, it would be reasonable to attempt to get such data, too, by using e.g. tracer particles with different X-ray absorption coefficients.

Acknowledgement

The authors would like to acknowledge the support of the Hungarian National Foundation for Fundamental Research (Grant No. OTKA T029313) and the help of Prof. G. I. Tardos, the City College of the City University of New York for his valuable advises in fulfilling this work.

References

1. Hounsfield, G. N.: Computerized transverse axial scanning (tomography). *Br. J. Radiol.*, **46** (1973) 1016-1022.
2. Honarpour, M. M., Cromwell, V., Hatton, D., Satchwell, R.: Reservoir rock descriptions using Computer Tomography. 60th Annual Technical Conference and Exhibition of SPE, 1985, Las Vegas.
3. Foldes, T., Argyelán, G., Kiss, B., Bogner, P., Repa, I.: Application of medical computer tomograph measurements in 3D reservoir characterization. Conference Volume of EAGE & SAID Conference, 2000, Paris.
4. Bartholomew, R. N., Casagrande, R. M.: Measuring solids concentration in fluidized systems by gamma-ray absorption. *Ind. Eng. Chem.*, **49** (1957) 428-431.

5. Martin, M. P. et al.: Gas and solid behavior in cracking circulating fluidized beds. *Powder Technol*., **70** (1992) 249-258.

6. Chester, A. W. et al: Mixing dynamics in catalyst impregnation in double-cone blenders. *Powder Technol.*, **102** (1999) 85-94.

7. Sederman, A. J., Alexander, P., Gladden, L. F.: Structure of packed beds probed by Magnetic Resonance Imaging. *Powder Technol.*, **117** (2001) 255-269.

8. Sederman, A. J., Johns, M. L., Bramley, A. S., Alexander, P., Gladden, L. F.: Magnetic resonance imaging of liquid flow and pore structure within packed beds. *Chem. Eng. Sci.*, **52** (1997) 2239-2250.

9. Sederman, A. J., Johns, M. L., Alexander, P., Gladden, L. F.: Structure-flow correlations in packed beds. *Chem. Eng. Sci.*, **53** (1998) 2117-2128.

10. George, D. L. et al.: Three-phase material distribution measurements in a vertical flow using gamma-densitometry tomography and electrical-impedance tomography. *Int. J. Multiphase Flow.*, **27** (2001) 1903-1930.

11. Mann, R. et al.: Development of mixing models using electrical resistance tomography. *Chem. Eng. Sci.*, **52** (1997) 2073-2085.

12. Mann, R. et al.: Application of electrical resistance tomography to interrogate mixing process at plant scale. *Chem. Eng. Sci.*, **52** (1997) 2087-2097.

13. Dyakowski, T., Jeanmeure, L. F. C., Jaworski A. J.: Application of electrical tomography for gas-solids and liquid-solids flows – a review. *Powder Technol.*, **112** (2000) 174-192.

14. McKee, S. L. et al.: Solids flow imaging and attrition studies in a pneumatic conveyor. *Powder Technol.*, **82** (1995) 105-113.

15. Ostrowski, K. et al.: Real time visualisation and analysis of dense phase powder conveying. *Powder Technol.*, **102** (1999) 1-13.

16. York, T. A. et al.: Particle detection using integrated capacitance sensor. *Sensors and Actuators A: Physical*., 12 (2001) 74-79.

17. Warsito, W., Fan, L.-S.: Measurement of real-time flow structures in gas-liquid and gas-liquid-solid flow system using electrical capacitance tomography (ECT). *Chem. Eng. Sci.*, **56** (2001) 6455-6462.

18. Schlaberg, H. I., Podd, F. J. W., Hoyle, B. S.: Ultrasound process tomography system for hydrocyclones. *Ultrasonics*. **38** (2000) 813-816.

19. Tardos, G. I., Khan, M. I., Schaeffer, D. G.: Forces on a slowly rotating rough cylinder in a Cuette device containing a dry, frictional powder, *Physics of Fluids*, **10** (3) (1998) 335.

20. Osiris Imaging Software, Version 3.1. User Manual. UINHCUG, Geneva, 1995-96.

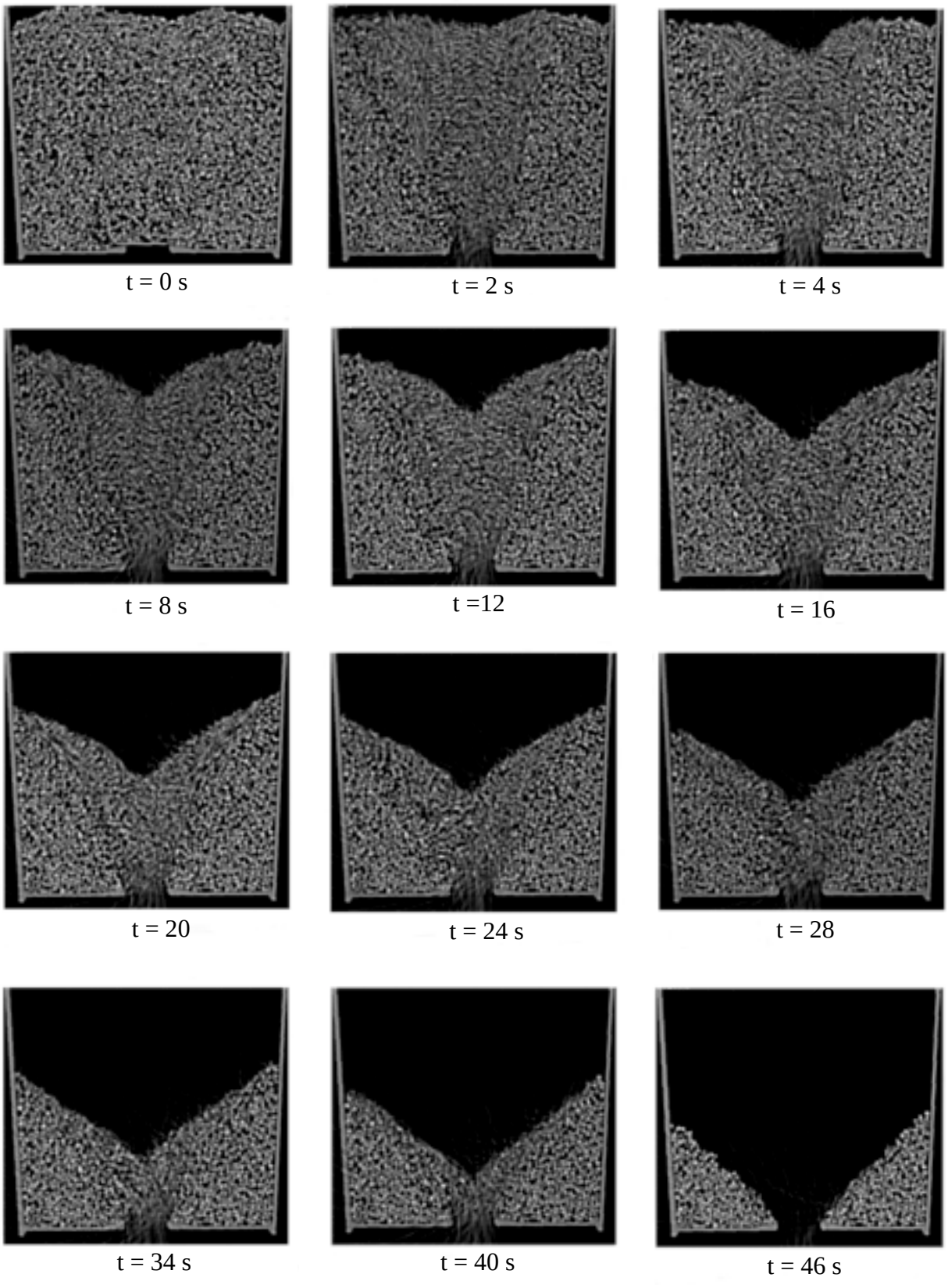

Figure 1.

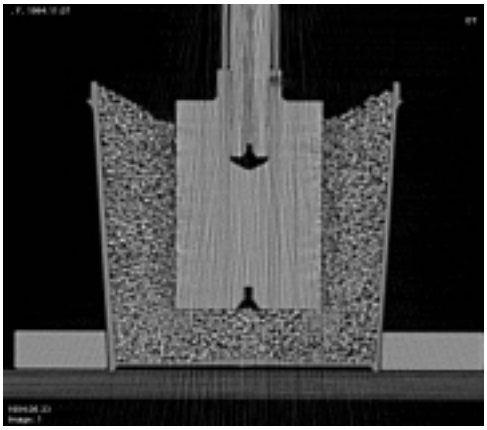

Figure 2.

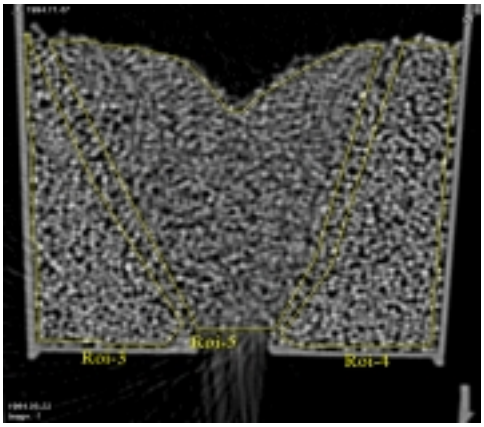

Figure 3.

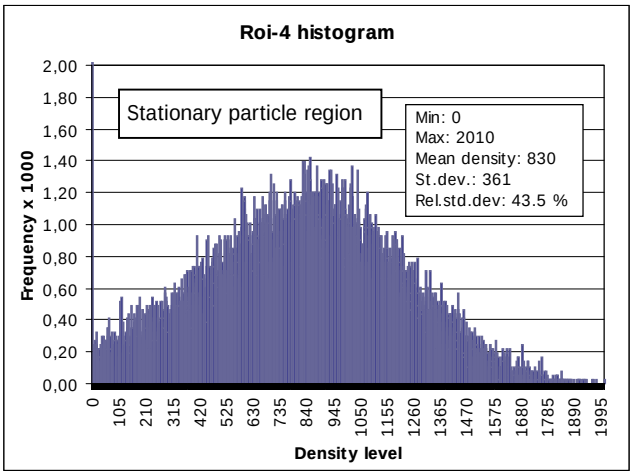

Figure 4a.

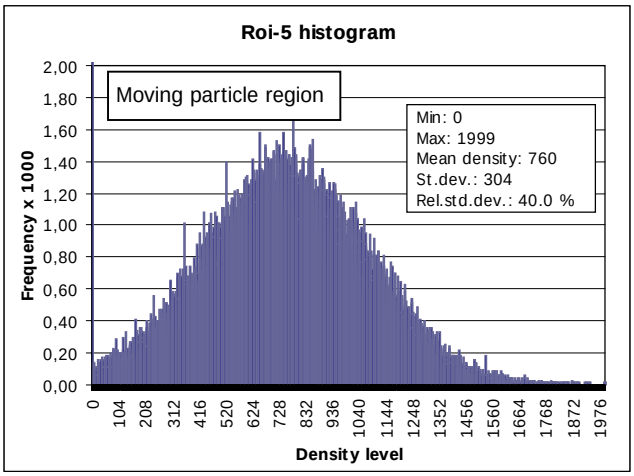

Figure 4b.

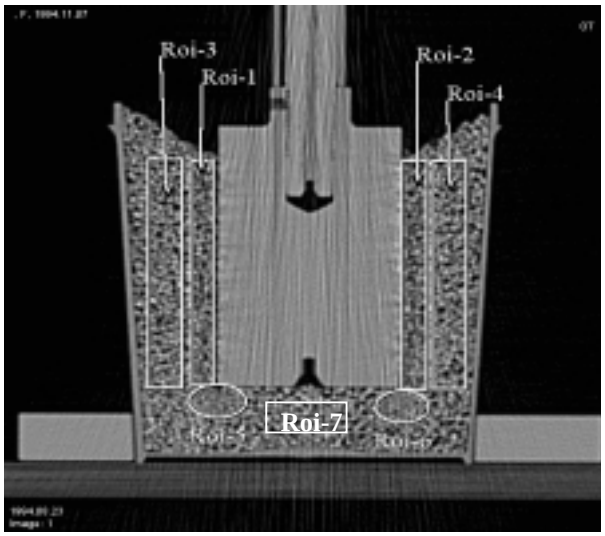

Figure 5

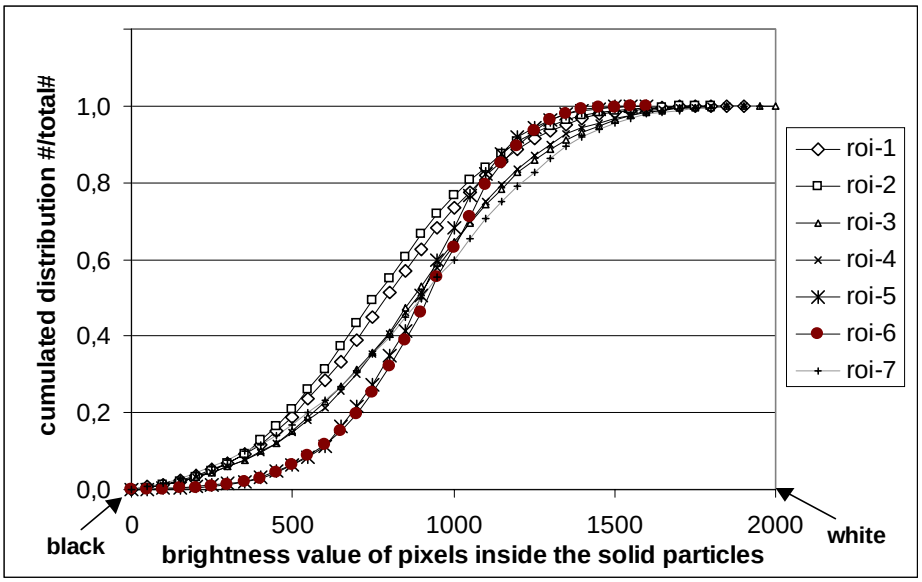

Figure 6

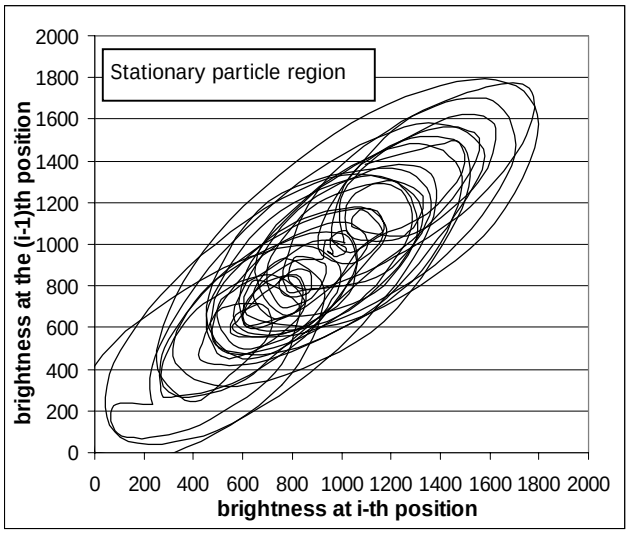

Figure 7a

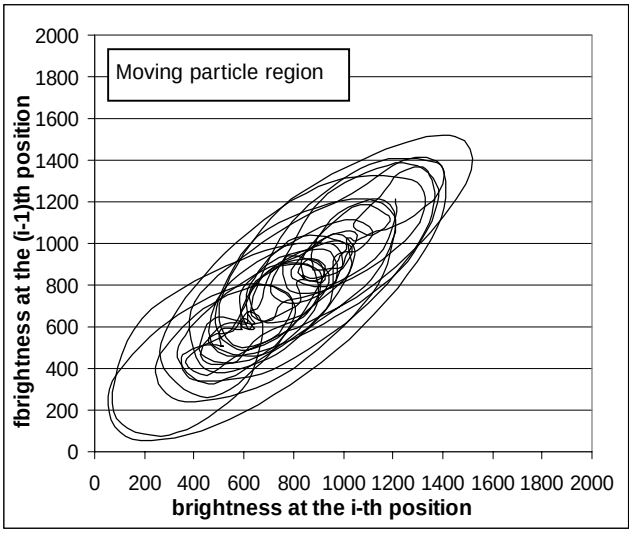

Figure 7b.